

# Philipps-Universität Marburg

Johannes Gille

Fachbereich 17

AG Allgemeine und Biologische Psychologie

AE Theoretische Kognitionswissenschaft

Learning in cortical microcircuits with multi-compartment pyramidal neurons

## **Supervisors:**

Prof. Dr. Dominik Endres, Philipps-Universität Marburg

Dr. Johan Kwisthout, Radboud University

# Contents

<b>1</b>	<b>Introduction</b>	<b>3</b>
1.1	Motivation . . . . .	3
1.2	The Backpropagation of errors algorithm . . . . .	3
1.2.1	Local error representation . . . . .	4
1.2.2	The weight transport problem . . . . .	4
1.2.3	Neuron models . . . . .	4
1.3	Approximations of the Backprop algorithm . . . . .	5
1.4	Cortical microcircuits . . . . .	6
<b>2</b>	<b>Methods</b>	<b>7</b>
2.1	Neuron and network model . . . . .	7
2.1.1	Network architecture . . . . .	7
2.1.2	Neuron models . . . . .	9
2.2	Urbanczik-Senn Plasticity . . . . .	10
2.3	The self-predicting network state . . . . .	11
	is there a mathematical symbol for this type of convergence? . . . . .	12
2.4	Training the network . . . . .	13
	what does the $O$ mean? . . . . .	13
2.5	The NEST simulator . . . . .	14
	cite this or nah? . . . . .	14
2.6	Neuron model implementation . . . . .	15
2.7	Event-based Urbanczik-Senn plasticity . . . . .	16
2.8	Neuron model adaptations . . . . .	21
2.9	Haider 2021 updates . . . . .	21
2.10	Latent equilibrium . . . . .	22
2.11	rate neurons in NEST . . . . .	22
2.12	simulation details/updates . . . . .	22
<b>3</b>	<b>Results</b>	<b>23</b>
3.1	direct feedback connections to interneurons . . . . .	23

3.2	Presentation times with latent equilibrium . . . . .	23
<b>4</b>	<b>room for random observations</b>	<b>25</b>
<b>5</b>	<b>Discussion</b>	<b>26</b>
5.1	Limitations of the implementation . . . . .	26
5.2	Whittington and Bogacz criteria . . . . .	26
5.3	Should it be considered pre-training? . . . . .	26
5.4	Relation to energy minimization . . . . .	27
5.5	Outlook . . . . .	27
<b>6</b>	<b>Appendix</b>	<b>28</b>
6.1	Somato-dendritic coupling . . . . .	28
6.2	Presentation times and Latent Equilibrium . . . . .	28
6.3	Parameter study . . . . .	31
<b>7</b>	<b>Preliminary structural components</b>	<b>33</b>
7.1	Synaptic delays . . . . .	33
7.2	Literature review - Backpropagation in SNN . . . . .	33
7.3	NEST Urbanczik-senn implementation . . . . .	33
7.4	My neuron model . . . . .	33
7.4.1	NEST rate neuron shenanigans . . . . .	33
7.5	My synapse model . . . . .	34
7.6	The relation between the pyramidal microcircuit and actual microcircuits . . .	34
7.6.1	Interneurons and their jobs . . . . .	34
7.7	Does it have to be backprop? . . . . .	34
7.8	Discrepancies between mathematica and NEST model . . . . .	34
7.9	Transfer functions . . . . .	34
<b>8</b>	<b>The weight-leakage tradeoff</b>	<b>35</b>
<b>9</b>	<b>Open Questions</b>	<b>36</b>

# Chapter 1

## Introduction

### 1.1 Motivation

**TODO: fill with citations?**

The outstanding learning capabilities of the human brain have been found to be elusive and as of yet impossible to replicate in silicio. While the power and utility of classical Machine-learning solutions has improved greatly in recent years, these approaches can not serve as an adequate model of human cognition. The sheer number of neurons and synapses in the brain makes simulations of an entire brain impossible with current hardware constraints. In fact, it has been found to be a substantial challenge to create artificial neural networks that simulate even parts of human neurophysiology while simultaneously being able to learn in a goal-oriented way.

The literature entails numerous approaches to address this challenge, with varying degrees of success. In this thesis, I will investigate one such approach, and attempt to modify it in a way that it more closely resembles properties exhibited by the human neocortex.

**TODO: eigentvalue of the hessian matrix. if they have different signs, something might be off**

### 1.2 The Backpropagation of errors algorithm

The Backpropagation of errors algorithm (henceforth referred as "Backprop") forms the backbone of modern machine learning. **TODO: cite** It is as of yet unmatched with regard to training in deep neural networks due to its unique capability to attribute errors in the output of a network to activations of specific neurons within its hidden layers and adapt incoming weights in order to improve network performance. This property also forms the basis of the algorithm's name; After an initial forward pass to form a prediction about the nature of a given input, a separate backward pass propagates the arising error through all layers in reverse order. During this second network traversal, local error gradients dictate, to what extent a

given weight needs to be altered so that the next presentation of the same sample would elicit a lower error in the output layer.

While Backprop continues to prove exceptionally useful in conventional machine learning systems, attempts use it to explain the exceptional learning capabilities of the human brain have so far not been successful **phrasing**. In fact, Backprop as a mechanism for synaptic plasticity in the brain is dismissed by many neuroscientists as biologically implausible. This dismissal is often focussed on three mechanisms that are instrumental for Backprop (Whittington and Bogacz, 2019; Crick, 1989; Bengio et al., 2015):

### 1.2.1 Local error representation

Within conventional artificial neural networks (ANNs), the neurons only serve the purpose of transmitting signals in a feedforward fashion. The errors on the other hand are computed and propagated by a completely separate algorithm which can access the entirety of the network state. The algorithm requires the activation of all downstream neurons in order to compute the weight changes of a given layer. Since plasticity in biological neurons is only dependent on factors that are local to the synapse, these errors would need to be represented within the neurons of each layer. Several mechanisms have been proposed to do this in a biologically plausible way, which will be discussed **TODO: in a later chapter**.

### 1.2.2 The weight transport problem

During the weight update stage of Backprop, errors are transmitted between layers with the same weights that are used in the forward pass. In other words, the magnitude of a neuron-specific error that is propagated through a given connection should be proportional to its impact on output loss during the forward pass. For this to work, a neuronal network would require feedback connections that mirror both the network structure and synaptic weights exhibited by the original network. It was long assumed that the feedback weights are required to be an exact match, but Liao et al. (2016) showed, that this constraint can be relaxed somewhat to a concordance of weight signs.

Bidirectional connections are common in the cortex, yet it is unclear by which mechanism pairs of synapses would be able to align. This issue becomes particularly apparent when considering long-range pyramidal projections, in which feedforward and feedback synapses would be separated by a considerable distance.

Several theories have been proposed as to how biological neural networks could alleviate this issue, which will be discussed **TODO: in a later section**.

### 1.2.3 Neuron models

While the fundamental computational unit of ANNs is called a neuron, it usually shares little resemblance to biological neurons. Most notably, these types of artificial neurons transmit a

continuous activation. In theory, these activations correspond to the firing rate of a spiking neuron. Yet particularly with regard to synaptic plasticity, spike based communication poses a substantial challenge. Plasticity rules derived for rate neurons do not necessarily have an easily derived counterpart for spiking neurons. A notable example for this issue is Backprop itself; The local error gradient  $\frac{\delta E}{\delta \phi(u_i)}$  **TODO: cleanup** requires a method of filtering the spiketrain which itself has no derivative **phrasing...**

To differentiate the two, I will be following Haider et al. (2021) in this Thesis; When referring to biologically plausible, leaky neurons I will be using the term "*neuronal*". Respectively, when discussing abstract neurons with instantaneous response, I will be using "*neural*".

Furthermore, a given neuron's activation is computed from a simple weighted sum of all inputs. This fails to capture the complex nonlinearities of synaptic connections that appear to be critical for neuronal computation. Finally, these abstract neurons - at least in classical Backprop - have no persistence through time. Thus, their activation is dictated strictly by the presentation of a single stimulus, in contrast to the leaky membrane dynamics exhibited by biological neurons. **TODO: talk about multiplicity of possible neuron models?**

### Transitioning to spiking neurons

It should also be noted that neuroscience has produced a vast amount of results which imply that the brain relies on precise spike timing for its plasticity **TODO: cite**. Thus, one might expect rate neuron approximations to underperform compared to spiking neurons, since a spiketrain contains more information than a rate approximation. However, several studies describe the opposite effect: Spiking neurons often perform substantially worse on learning tasks when compared to rate neurons with similar plasticity rules (Stapmanns et al., 2021) **TODO: cite more**. Given this data I assume that my implementation will also perform slightly worse than the existing rate implementations.

**TODO: discuss supervisor issue?**

## 1.3 Approximations of the Backprop algorithm

These results have largely led neuroscience to dismiss Backprop as a plausible learning mechanism for biological brains, and focus different learning mechanisms **TODO: do some reading and expand this**. Yet, Backprop has remained the gold standard against which all supervised learning mechanisms eventually have to compare.

And despite its apparent biological implausibility, it does share some notable parallels to learning in the brain: When training on real-world data, artificial neural networks have been shown to learn similar representations as those found in brain areas responsible for comparable tasks Whittington and Bogacz (2019); Yamins and DiCarlo (2016). **TODO: talk about ideal observer?**

Thus, several attempts have been made to find biologically more plausible approximations of Backprop, which will be discussed in this section.

## **1.4 Cortical microcircuits**

# Chapter 2

## Methods

### 2.1 Neuron and network model

This section will go into detail about the computations behind the network which was developed by Sacramento et al. (2018) and expanded by Haider et al. (2021).

#### 2.1.1 Network architecture

The model which was original described by Sacramento et al. (2018) contains a strongly recurrent network structure, which will be explained in this section. It can be functionally separated into layers, with information flowing from the input layer through one or more hidden layers to the output layer. Neurons at the input layer receive no feedback connections and serve primarily to apply a low-pass filter over the input sequence injected into their membrane. Output layers have no interneurons, and are usually modeled as pyramidal neurons without an apical compartment. Hidden layers consist of a pyramidal- and an interneuron population, which are fully connected to each other in both directions (see Figure 2.1). Feedforward connections between layers are facilitated by all-to-all connections between their respective pyramidal neurons and innervate the basal compartments. Feedback connections from superficial layers and interneurons on the other hand arrive at apical compartments. Interneurons receive lateral input from all pyramidal neurons of their layer, as well as feedback information from superficial pyramidal neurons. These feedback connections are special, since they connect one pyramidal neuron to exactly one interneuron. Instead of transmitting neuronal activation, this connection relays somatic voltage directly. The resulting dynamics share features of electrical synapses, which will be discussed in Section 3.1. To understand what purpose this connectivity serves in our model, neuron and plasticity models require some elaboration.

---

<sup>1</sup>Note that the input layer is displayed as having interneurons here. This appears to be a mistake in the graphic. In the implementation, interneurons are only modelled in hidden layers.



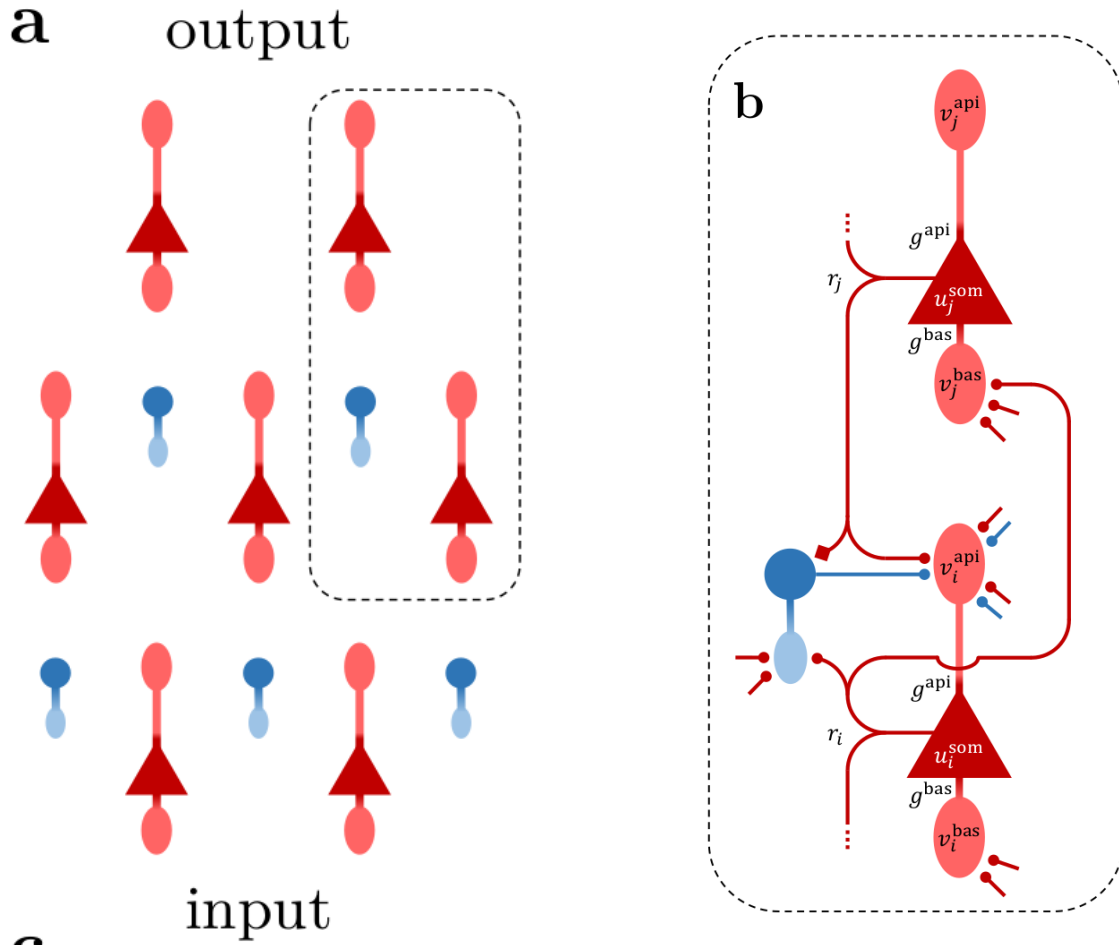


**Figure 2.1:** Network structure, from Haider et al. (2021). **a:** pyramidal- (red) and interneurons (blue) in a network of three layers. Note the fact that the number interneurons in a layer is equal to the number of pyramidal neurons in the subsequent layer<sup>1</sup>. **b:** connectivity within the highlighted section. Feedback pyramidal-to-interneuron connections (displayed with rectangular synapse) transmit pyramidal somatic potential directly and connect to a single interneuron. This enables these interneurons to learn to match their corresponding next-layer pyramidal neurons. All other synapses (circles) transmit the neuron somatic activation  $\phi(u^{\text{som}})$  and fully connect their origin and target populations.

### 2.1.2 Neuron models

The network contains two types of multi-compartment neurons; Pyramidal neurons with three compartments each, and interneurons with two compartments each. They integrate synaptic inputs into dendritic potentials, which leak into the soma with specific conductances. Note that vector notation will be used throughout this section, and  $u_l^P$  and  $u_l^I$  denote the column vectors of pyramidal- and interneuron somatic voltages respectively. Synaptic weights  $W$  are likewise assumed matrices. The activation  $r_l^P$  of pyramidal neurons at layer  $l$  is given by applying the synaptic transfer function  $\phi$  to their somatic potentials  $u_l^P$ :

$$r_l^P = \phi(u_l^P) \quad (2.1)$$

$$\phi(x) = \begin{cases} 0 & \text{if } x < -\varepsilon \\ \gamma \log(1 + e^{\beta(x-\theta)}) & \text{if } -\varepsilon \leq x < \varepsilon \\ \gamma x & \text{otherwise} \end{cases} \quad (2.2)$$

where  $\phi$  acts componentwise on  $u$  and can be interpreted as a smoothed variant of ReLU **TODO: cite** with scaling factors  $\gamma$ ,  $\beta$ ,  $\theta$  and threshold parameter  $\varepsilon$ . The derivative somatic membrane potentials of layer  $l$  pyramidal neurons is given by:

$$C_m \dot{u}_l^P = -g_l u_l^{som} + g^{bas} v_l^{bas} + g^{api} v_l^{api} \quad (2.3)$$

where  $v_i^{bas}$  and  $v_i^{api}$  are the membrane potentials of basal and apical dendrites respectively, and  $g^{bas}$  and  $g^{api}$  their corresponding coupling conductances. The membrane capacitance  $C_m$  is 1 in all relevant simulations, and will be omitted from all Equations from here on out.

In the original model, dendritic compartments have no persistence between simulation steps. Thus, they are defined at every timestep  $t$  through incoming weight matrices and presynaptic activities:

$$v_l^{bas}(t) = W_l^{up} \phi(u_{l-1}^P(t)) \quad (2.4)$$

$$v_l^{api}(t) = W_l^{pi} \phi(u_l^I(t)) + W_l^{down} \phi(u_{l+1}^P(t)) \quad (2.5)$$

Weight nomenclature conforms to the python implementation of the network by Haider et al. (2021); Weights are indexed by the layer in which the target neuron is located and belong to one of four populations. Feedforward and feedback pyramidal-to-pyramidal connections arriving at layer  $l$  are denoted  $W_l^{up}$  and  $W_l^{down}$  respectively. Lateral pyramidal-to-interneuron connections are denoted with  $W_l^{ip}$  and their corresponding feedback connections with  $W_l^{pi}$ . Since the input layer contains no synapses, indexing begins with 0 for the first hidden layer.

Interneurons integrate synaptic information by largely the same principle, but instead of feedback information arriving at the apical compartment, it is integrated directly into the soma. Through this, interneurons functionally resemble the original neuron from Urbanczik and Senn (2014) most closely.

$$C_m \dot{u}_l^I = -g_l u_l^I + g^{dend} v_l^{dend} + i^{nudge,I} \quad (2.6)$$

$$i^{nudge,I} = g^{nudge,I} u_{l+1}^P \quad (2.7)$$

$$v_l^{dend} = W_l^{ip} \phi(u_l^P) \quad (2.8)$$

where  $g^{nudge,I}$  is the interneuron nudging conductance, and  $u_{l+1}^P$  is the somatic voltage of a corresponding pyramidal neuron in the next layer. Since each interneuron is innervated by exactly one pyramidal neuron and vice versa, they will be called each others **sister neurons** from here on. **TODO: discuss whether this 1 to 1 style connection is plausible!** Pyramidal neurons in the output layer  $N$  effectively behave like interneurons, as they receive no input to their apical compartment. Instead, the target activation  $u^{tgt}$  is injected into their soma:

$$C_m \dot{u}_N^P = -g_N u_N^P + g^{bas} v_N^{bas} + i^{nudge,tgt} \quad (2.9)$$

$$i^{nudge,tgt} = g^{nudge,tgt} u^{tgt} \quad (2.10)$$

These neuron dynamics correspond closely to those by Urbanczik and Senn (2014), including the extension to more than two compartments which was proposed in the paper. It should be noted however, that they are simplified in some key ways. Primarily, dendritic couplings and nudging are not relative to the somatic or some reversal potential (i.e.  $i^{nudge,tgt} = g^{nudge,tgt} (u^{tgt} - u_N^P)$ ), but are simplified to absolute values. **TODO: Figure out if this makes a difference. maybe create a second branch to try them out?**

## 2.2 Urbanczik-Senn Plasticity

The synapses in the network are all modulated according to variations of the "Urbanczik-Senn" plasticity rule (Urbanczik and Senn, 2014), which will be discussed in this section. **TODO: add paragraph about relevance of urbanczik-senn**

The plasticity rule requires the postsynaptic neuron to have one somatic and at least one dendritic compartment, to the latter of which synapses connect. The membrane potential of the dendritic compartment leaks into the somatic compartment as described in Equation 2.6.

Functionally, the plasticity rule changes the synaptic weight in such a way, as to minimize discrepancies between somatic and dendritic potential. The change in weight for a synapse

from neuron  $j$  to neuron  $i$  is thus given by:

$$\dot{w}_{ij} = \eta (\phi(u_i^{som}) - \phi(\hat{v}_i^{bas})) \phi(u_j^{som})^T \quad (2.11)$$

$$\hat{v}_i^{bas} = \alpha v_i^{bas} \quad (2.12)$$

with learning rate  $\eta$  and  $u^T$  denoting the transposition of the vector  $u$  (which is by default assumed to be a column vector). The dendritic prediction is simply a scaled version of the dendritic potential by the constant factor  $\alpha$ , which is calculated from coupling and leakage conductances. For example, basal dendrites of pyramidal neurons in Sacramento et al. (2018) are attenuated by  $\alpha = \frac{g^{bas}}{g_l + g^{bas} + g^{api}}$ . If a current is injected into the soma, it creates a difference between somatic firing rate and dendritic prediction (referred to as a dendritic error from here on). Urbanczik and Senn (2014) show, that **TODO: what?**

Weight changes for the synapses in a hidden layer  $l$  are thus given by:

$$\dot{w}_l^{up} = \eta_l^{up} (\phi(u_l^P) - \phi(\hat{v}_l^{bas})) \phi(u_{l-1}^P)^T \quad (2.13)$$

$$\dot{w}_l^{ip} = \eta_l^{ip} (\phi(u_l^I) - \phi(\hat{v}_l^{dend})) \phi(u_l^P)^T \quad (2.14)$$

$$\dot{w}_l^{pi} = \eta_l^{pi} - v_l^{api} \phi(u_l^I)^T \quad (2.15)$$

$$\dot{w}_l^{down} = \eta_l^{down} (\phi(u_l^P) - \phi(\hat{v}_l^{api})) \phi(u_{l+1}^P)^T \quad (2.16)$$

Note that pyramidal-to-pyramidal feedback weights  $w_l^{down}$  are not plastic in most simulations, and are only listed here for the sake of completeness **TODO: some notes in the appendix to this?**

## 2.3 The self-predicting network state

In this model, euron dynamics, plasticity rules and network architecture form an elegant interplay, which I expand on in this section. We will

Since each interneuron receives a somatic nudging signal from its corresponding next-layer pyramidal neuron, incoming synapses from lateral pyramidal neurons adapt their weights to match feedforward pyramidal-to-pyramidal weights. In intuitive terms; Feedforward pyramidal-to-pyramidal weights elicit a certain activation in the subsequent layer, which is fed back into corresponding interneurons. In order to minimize the dendritic error term in Equation 2.14, pyramidal-to-interneuron weight matrices at every layer must match these forward weights ( $w_l^{ip} \approx \rho w_l^{up}$ ) up to some scaling factor  $\rho$ .  $\rho$  depends on the difference in parameters between pyramidal- and interneurons, and is close to 1 for most of the simulations considered here. As long as no feedback information arrives at the pyramidal neurons, the Urbanczik-Senn plasticity drives synaptic weight to fulfill this constraint. Note, that this alignment of two separate

sets of outgoing weights is achieved with only local information. Therefore this mechanism could plausibly align the weights of biological synapses that are physically separated by long distances.

Next, consider the special case for interneuron-to-pyramidal weights in Equation 2.15, in which plasticity does not serve to reduce discrepancies between dendritic and somatic potential. The error term is instead defined solely by the apical compartment voltage<sup>2</sup>. Thus, plasticity in these synapses works towards silencing the apical compartment. The apical compartments also receive feedback from superficial pyramidal neurons, whose synapses will be considered non-plastic for now. As shown above, interneurons each learn to match their respective sister neuron activity. Thus, silencing of apical compartments can only be achieved by mirroring the pyramidal-to-pyramidal feedback weights ( $w_l^{pi} \approx -w_l^{down}$ ).

When enabling plasticity in only these two synapse types, the network converges on the "self-predicting state" (Sacramento et al., 2018). This state is defined by a minimization of four error metrics at each hidden layer  $l$ :

- The symmetries between feedforward ( $w_l^{ip} \approx \rho w_l^{up}$ ) and feedback ( $w_l^{pi} \approx -w_l^{down}$ ) weights. Mean squared error between these pairs of matrices will be called **Feedforward - and Feedback weight error** respectively.
- Silencing of pyramidal neuron apical compartments ( $v_l^{api} \approx 0$ ). The Frobenius norm **TODO: cite** of apical compartment voltages within a layer is called the **Apical error**.
- Equal activations in interneurons and their respective sister neurons ( $\phi(u_l^I) \approx \phi(u_{l+1}^P)$ ). The mean squared error over these vectors is called the **Interneuron error**.

### is there a mathematical symbol for this type of convergence?

All of these equalities are approximate, since the network does not ever reach a state in which all of these values are zero. In the original implementation, these deviations are minute and can likely be explained with floating point conversions. Since it is impossible to replicate the timing of the original precisely within NEST, the NEST simulations deviate more strongly from this ideal. The key insight here is, that this state is not clearly defined by absolute error thresholds, but is rather flexible. Thus, networks are able to learn successfully even when their weights are initialized imperfectly. **TODO: or not at all? some science is required here**

An analysis of the equations describing the network reveals that the self-predicting state is stable **phrasing**. When Interneuron error is zero, dendritic and somatic compartments of all interneurons are equal, thus effectively disabling plasticity in incoming synapses. Likewise, a silenced apical compartment will disable plasticity in all incoming synapses. Synapses from

---

<sup>2</sup>In strict terms, it is defined by the deviation of the dendritic potential from its specific reversal potential. Since that potential is zero throughout,  $-v_l^{api}$  remains as the error term.

lateral interneurons (Equation 2.15) only depend on the apical compartment itself, thus can not change in this state. Similarly, the apical compartment is also the driving factor for the dendritic error of feedforward synapses (Equation 2.13), since it affects somatic activity when active<sup>3</sup>. Thus, all plasticity in the network is disabled, and remains in the self-predicting state regardless of the kind of stimulus injected into the input layer. This fact highlights another important property of networks in this state. Notice, how information flows backwards through the network; All feedback signals between layers ultimately pass through the apical compartments of pyramidal neurons. Thus, successful silencing of all apical compartments implies that no information can travel backwards between layers (with the exception of interneurons receiving top down signals). As a result, the network behaves strictly like a fully connected feedforward network consisting only of pyramidal neurons. The recurrence within this network is in balance, and completely cancels out its own effects. This holds true as long as all conditions for the self-predicting state are fulfilled, and the network only receives external stimulation at the input layer. One interpretation of this is, that the network has learned to predict its own top-down input. A failure by interneurons to fully explain (i.e. cancel out) top-down input thus results in a prediction error, encoded in deviation of apical dendrite potentials from their resting state. This prediction error in turn elicits plasticity in all synapses connecting to its pyramidal neuron, which drives the network towards a self-predicting state that is congruent with the novel top-down signal. Therefore, these neuron-specific prediction errors are the driving force of supervised learning in these networks

## 2.4 Training the network

Starting with a network in the self-predicting state, performing time-continuous supervised learning then requires an injection of a target activation into the network's output layer alongside with a stimulus at the input layer. Since output layer neurons feed back into both interneurons and pyramidal neurons of the previous layer, local prediction errors arise. Synapses activate and drive to minimize the prediction errors, which requires the network to replicate the target activation from activations and weights of the last hidden layer.

Note, that this mechanism is not exclusive to the last two layers. Any Apical errors cause a change in somatic activity, which previous layers will fail to predict. Thus, errors are propagated backwards through the entire network, causing error minimization at every layer. See the Supplementary analysis of Sacramento et al. (2018) for a rigorous proof that this type of network does indeed approximate the Backpropagation algorithm **what does the  $O$  mean?** .

---

<sup>3</sup>This feature is actually rather important when contemplating biological neurons using the Urbanczik-Senn plasticity. In the original paper, currents were injected directly into the soma to change the error term. The introduction of a second dendrite which performs that very task is much more useful, as originally described by the authors. Whether interneurons could be modeled by the same principles will be discussed in Section **TODO: talk about interneuron dendritic trees**

Classical backpropagation relies on a strict separation of a forward pass of some training pattern and a backwards pass dependent on the loss produced at the output layer. Since this network is time-continuous, stimulus and target activation are injected into the network simultaneously. These injections are maintained for a given presentation time  $t_{pres}$ , in order to allow the network to calculate errors through its recurrent connections before slowly adapting weights. Particularly for deep networks, signals travelling from both the input and output layer require some time to balance out and elicit the correct dendritic error terms. The network tends to overshoot activations, which in turn can lead to poor learning performance with high learning rates. This issue will be discussed in more detail in Section 2.9.

## 2.5 The NEST simulator

One of the key research questions motivating this thesis is whether the proposed architecture would be able to learn successfully when employing spike-based communication instead of the rate connections for which the original implementation was developed. As a framework for my spike-based implementation two options were considered: The first one was to use the existing implementation of the network within PyTorch **cite this or nah?** and expand it to employ spiking neurons. PyTorch does in principle support spiking communication between layers, but is streamlined for implementing less recurrent and less complex network and neuron models. A more pressing issue yet is efficiency; PyTorch is very well optimized for efficiently computing matrix operations on dedicated hardware. This makes it a prime choice for simulating large networks of rate neurons, which transmit all of their activations between layers at every simulation step. Spiking communication between leaky neurons is almost antithetical to this design philosophy and thus can be expected to perform comparatively poor when using this backend.

The second option was to use the NEST simulator **TODO: cite**, which was developed with highly parallel simulations of large spiking neural networks in mind. It is written in C++ and uses the *Message Passing Interface* to efficiently communicate payloads across both threads and compute nodes. One design pillar of the simulator that is particularly relevant for this project, is the event-based communication scheme that underpins all simulated nodes. It ensures, that communication bandwidth at every simulation step is only used by the subset of nodes which transmit spikes or other signals at that time step. The simulator also increases computational efficiency by enforcing a transmission delay of at least one simulation step for all connections. This allows Events to be created out of order, and processed at the postsynaptic neuron during the next simulation step. While this feature is critical for efficiency in highly parallel environments, it inflicts some limitations on the simulation which will be discussed in **TODO: create section**. Yet the most notable advantage of the NEST simulator is, that an event-based implementation of the Urbanczik-Senn plasticity alongside a corresponding neuron model had already been developed for it. Combined with the fact that I had more

prior experience with NEST over PyTorch, I decided to implement the neuron model in the NEST simulator.

Early experiments showed that implementing a spiking neuron and synapse model that behave similarly enough to the original python implementation would be more challenging than expected. The interplay between neuron activity and synaptic plasticity proved to be very sensitive to minor differences in parametrization and simulator setup. It was also uncertain if spiking neurons would be able to perform the required types of learning at all. Finally, the NEST simulator itself imposes some limitations on the simulations, which could not be ruled out as being responsible for the failure of these early experiments. Therefore, I decided to recreate the existing rate neuron model within NEST as well as the spiking implementation. This substantially increased the complexity of my NEST implementation, but turned out to be a critical step towards successful learning using spiking neurons. It allowed me to reliably identify whether errors arose from using a different simulation backend, or from the transition to spiking neurons.

## 2.6 Neuron model implementation

The neuron model relies heavily on the one developed by Stapmanns et al. (2021), who showed that spiking neurons are able to learn tasks that were originally implemented for the rate neurons and synapses developed by Urbanczik and Senn (2014).

To calculate a number of spikes from the rate  $r = \phi(u)$ , a poisson point process was used:

$$P\{n \text{ spikes during } \Delta t\} = e^{-r\Delta t} \frac{(r\Delta t)^n}{n!} \quad (2.17)$$

$$\langle n \rangle = r \Delta t \quad (2.18)$$

**TODO: find a citation for this**

with number of spikes  $n$  and simulation timestep  $\Delta t$ , which will be assumed to be  $0.1ms$  from here on out. Within the code, true number of spikes during  $\Delta t$  is drawn from a poisson distribution with parameter  $\langle n \rangle$ . Note that this mechanism makes the assumption that more than one spike can occur per simulation step. NEST was developed with this possibility in mind, and handles such high rates without issue. Yet for the analysis with regard to biological plausibility, spiking behaviour with refractory periods might be useful. The probability of at least one spike occuring within the next simulation step thus is the inverse probability of no spike occuring. Entering  $n = 0$  into Equation 2.17, the probability of eliciting at least one spike within the next simulation step becomes:

$$P\{n \geq 1\} = 1 - e^{-r\Delta t} \quad (2.19)$$



After randomly drawing from this probability a spike is sent, and the spiking probability is set to 0 for the duration of the refractory period  $t_{ref}$ .

## 2.7 Event-based Urbanczik-Senn plasticity

One major challenge in implementing this architecture with spiking neurons is the Urbanczik-Senn plasticity as introduced in Section 2.2. This problem has been successfully solved in NEST by Stapmanns et al. (2021) for the two-compartment neurons described in Urbanczik and Senn (2014). This Section will discuss its algorithm and implementation.

Since it depends on pre- and postsynaptic information for all updates, one of two approaches is typically employed to compute it:

One option is to store all relevant state variables for every timestep in the synapse and update the synaptic weight whenever a spike is sent through the synapse. This is efficient in terms of computation time, since fewer computations are required per synapse. The major downside of the approach lies in memory efficiency; Every synapse potentially stores the history over several hundred simulation steps. In addition, every synapse innervating a given neuron would store its membrane potentials redundantly.

Another approach updates synaptic weights at every timestep. This requires very little memory, but substantially increases computation time. Importantly, it is poorly suited for asynchronous neuron simulations, as all synapses and their weights need to be updated at every simulation step sequentially for their target neuron. In particular for large networks and modern hardware solutions, asynchronous simulations have proven to be more efficient for many use cases **TODO: cite something by abigail**

Thus, a novel approach was developed by Stapmanns et al. (2021) for the NEST simulator, which will be explained in this section. In order to utilize the paralellization capabilities of NEST and spiking neural networks, transmitting the pre- and postsynaptic membrane potential is a poor choice. Thus, the error between somatic and dendritic activation is stored in the `urbanczik_history` of the postsynaptic neuron. Since it applies equally to all incoming synapses, redundant storage is avoided by storing an access counter alongside each entry. Whenever an incoming syna

$$\kappa(t) = H(t)e^{-t/\tau_\kappa} \quad (2.20)$$

$$H(t) = \begin{cases} 1 & \text{if } t > 0 \\ 0 & \text{if } t \leq 0 \end{cases} \quad (2.21)$$

Antiderivatives:

$$\int_{-\infty}^x H(t)dt = tH(t) = \max(0, t) \quad (2.22)$$

Convolution:

$$(f * g)(t) = \int_{-\infty}^{\infty} f(\tau)g(t - \tau)d\tau \quad (2.23)$$

For functions  $f, g$  supported on only  $[0, \infty]$  (as one-sided decay kernels and spiketrains are), integration limits can be truncated:

$$(f * g)(t) = \int_0^t f(\tau)g(t - \tau)d\tau \quad (2.24)$$

$$(2.25)$$

Plasticity:

$$\frac{dW_{ij}}{dt}(t) = F(W_{ij}(t), s_i^*(t), s_j^*(t), V_i^*(t)) \quad (2.26)$$

$$F[s_j^*, V_i^*] = \eta \kappa * (V_i^* s_j^*) \quad (2.27)$$

$$\text{with } V_i^* = (s_i - \phi(V_i))h(V_i), \quad (2.28)$$

$$s_j^* = \kappa_s * s_j. \quad (2.29)$$

For an event-based plasticity we need:

$$\Delta W_{ij}(t, T) = \int_t^T dt' F[s_j^*, V_i^*](t') \quad (2.30)$$

$$= \int_t^T dt' \eta \kappa * (V_i^* s_j^*) \quad (2.31)$$

$$= \eta \int_t^T dt' \int_0^{t'} dt'' \kappa(t' - t'') V_i^*(t'') s_j^*(t'') \quad (2.32)$$

$$= \eta \int_0^t dt' \int_{t''}^{t'} dt'' \kappa(t' - t'') V_i^*(t'') s_j^*(t'') \quad (2.33)$$

$$(2.34)$$

Starting with the complete Integral from  $t = 0$ .

$$\Delta W_{ij}(0, t) = \eta \int_0^t dt' \int_0^{t'} dt'' \kappa(t' - t'') V_i^*(t'') s_j^*(t'') \quad (2.35)$$

$$= \eta \int_0^t dt'' \int_{t''}^t dt' \kappa(t' - t'') V_i^*(t'') s_j^*(t'') \quad (2.36)$$

$$= \eta \int_0^t dt'' [\tilde{\kappa}(t - t'') - \tilde{\kappa}(0)] V_i^*(t'') s_j^*(t'') \quad (2.37)$$

$$(2.38)$$

With  $\tilde{\kappa}$  being the antiderivative of  $\kappa$ :

$$\kappa(t) = \frac{\delta}{\delta t} \tilde{\kappa}(t) \quad (2.39)$$

$$\tilde{\kappa}(t) = -e^{-\frac{t}{\tau\kappa}} \quad (2.40)$$

$$(2.41)$$

The above can be split up into two separate integrals:

$$\Delta W_{ij}(0, t) = \eta [-I_2(0, t) + I_1(0, t)] \quad (2.42)$$

$$I_1(t_1, t_2) = - \int_{t_1}^{t_2} dt' \tilde{\kappa}(0) V_i^*(t') s_j^*(t') \quad (2.43)$$

$$I_2(t_1, t_2) = - \int_{t_1}^{t_2} dt' \tilde{\kappa}(t_2 - t') V_i^*(t') s_j^*(t') \quad (2.44)$$

$$(2.45)$$

Which implies the identities

$$I_1(t_1, t_2 + \Delta t) = I_1(t_1, t_2) + I_1(t_2, t_2 + \Delta t) \quad (2.46)$$

$$I_2(t_1, t_2 + \Delta t) = e^{-\frac{t_2 - t_1}{\tau\kappa}} I_2(t_1, t_2) + I_2(t_2, t_2 + \Delta t) \quad (2.47)$$

$$I_2(t_1, t_2 + \Delta t) = - \int_{t_1}^{t_2 + \Delta t} dt' \tilde{\kappa}(t_2 + \Delta t - t') V_i^*(t') s_j^*(t') \quad (2.48)$$

$$= - \int_{t_1}^{t_2} dt' \left[ -e^{-\frac{t_2 + \Delta t - t'}{\tau_\kappa}} \right] V_i^*(t') s_j^*(t') - \int_{t_2}^{t_2 + \Delta t} dt' \left[ -e^{-\frac{t_2 + \Delta t - t'}{\tau_\kappa}} \right] V_i^*(t') s_j^*(t') \quad (2.49)$$

$$= -e^{-\frac{\Delta t}{\tau_\kappa}} \int_{t_1}^{t_2} dt' \left[ -e^{-\frac{t_2 - t'}{\tau_\kappa}} \right] V_i^*(t') s_j^*(t') - \int_{t_2}^{t_2 + \Delta t} dt' \left[ -e^{-\frac{t_2 + \Delta t - t'}{\tau_\kappa}} \right] V_i^*(t') s_j^*(t') \quad (2.50)$$

Using this we can rewrite the weight change from  $t$  to  $T$  as:

$$\Delta W_{ij}(t, T) = \Delta W_{ij}(0, T) - \Delta W_{ij}(0, t) \quad (2.51)$$

$$= \eta [-I_2(0, T) + I_1(0, T) + I_2(0, t) - I_1(0, t)] \quad (2.52)$$

$$= \eta [I_1(t, T) - I_2(t, T) + I_2(0, t) \left(1 - e^{-\frac{T-t}{\tau_\kappa}}\right)] \quad (2.53)$$

The simplified Sacramento et al. (2018) case would be:

$$\frac{dW_{ij}}{dt} = \eta (\phi(u_i) - \phi(\hat{v}_i)) \phi(u_j) \quad (2.54)$$

$$\Delta W_{ij}(t, T) = \int_t^T dt' \eta (\phi(u_i^{t'}) - \phi(\hat{v}_i^{t'})) \phi(u_j^{t'}) \quad (2.55)$$

$$\Delta W_{ij}(t, T) = \eta \int_t^T dt' (\phi(u_i^{t'}) - \phi(\hat{v}_i^{t'})) \phi(u_j^{t'}) \quad (2.56)$$

$$V_i^* = \phi(u_i^{t'}) - \phi(\hat{v}_i^{t'}) \quad (2.57)$$

$$s_j^* = \kappa_s * s_j \quad (2.58)$$

Where  $s_i$  is the postsynaptic spiketrain and  $V_i^*$  is the error between dendritic prediction and somatic rate and  $h(u)$ . The additional nonlinearity  $h(u) = \frac{d}{du} \ln \phi(u)$  is omitted in our model **TODO: should it though?**.

$$\tau_l = \frac{C_m}{g_L} = 10 \quad (2.59)$$

$$\tau_s = 3 \quad (2.60)$$

Writing membrane potential to history (happens at every update step of the postsynaptic neuron):

```

2 UrbanczikArchivingNode< urbanczik_parameters >::write_urbanczik_history(Time t
  , double V_W, int n_spikes, int comp)
3 {
4   double V_W_star = ( ( E_L * g_L + V_W * g_D ) / ( g_D + g_L ) );
5   double dPI = ( n_spikes - phi( V_W_star ) * Time::get_resolution().get_ms()
6     )
7     * h( V_W_star );
8 }

```

I interpret this as:

$$\int_{t_{ls}}^T dt' V_i^* = \int_{t_{ls}}^T dt' (s_i - \phi(V_i))h(V_i), \quad (2.61)$$

$$\int_{t_{ls}}^T dt' V_i^* = \sum_{t=t_{ls}}^T (s_i(t) - \phi(V_i^t)\Delta t)h(V_i^t) \quad (2.62)$$

$$(2.63)$$

```

1 for (t = t_ls; t < T; t = t + delta_t)
2 {
3   minus_delta_t = t_ls - t;
4   minus_t_down = t - T;
5   PI = ( kappa_l * exp( minus_delta_t / tau_L ) - kappa_s * exp(
6     minus_delta_t / tau_s ) ) * V_star(t);
7   PI_integral_ += PI;
8   dPI_exp_integral += exp( minus_t_down / tau_Delta_ ) * PI;
9 }
10 // I_2 (t,T) = I_2(0,t) * exp(-(T-t)/tau) + I_2(t,T)
11 PI_exp_integral_ = (exp((t_ls-T)/tau_Delta_) * PI_exp_integral_ +
12   dPI_exp_integral);
13 W_ji = PI_integral_ - PI_exp_integral_;
14 W_ji = init_weight_ + W_ji * 15.0 * C_m * tau_s * eta_ / ( g_L * ( tau_L -
15   tau_s ) );
16
17 kappa_l = kappa_l * exp((t_ls - T)/tau_L) + 1.0;
18 kappa_s = kappa_s * exp((t_ls - T)/tau_s) + 1.0;
19

```

$$\int_{t_{ls}}^T dt' s_j^* = \tilde{\kappa}_L(t') * s_j - \tilde{\kappa}_s(t') * s_j \quad (2.64)$$

$I_1$  in the code is computed as a sum:

$$I_1(t, T) = \sum_{t'=t}^T (s_L^*(t') - s_s^*(t')) * V^*(t') \quad (2.65)$$

## 2.8 Neuron model adaptations

- additional compartments
- top-down plasticity changes
- leaky dendrites
- pyr and intn differences
- 

$$u_k^p = \frac{g_B}{g_{lk} + g_B + g_A} v_{B,k}^p + \frac{g_A}{g_{lk} + g_B + g_A} v_{A,k}^p \quad (2.66)$$

$$\hat{v}_{B,k}^p = \frac{g_B}{g_{lk} + g_B + g_A} v_{B,k}^p \quad (2.67)$$

$$\hat{v}_k^I = \frac{g_B}{g_{lk} + g_B} v_k^I \quad (2.68)$$

$$\lambda = \frac{g_{som}}{g_{lk} + g_B + g_{som}} \quad (2.69)$$

## 2.9 Haider 2021 updates

Besides the using a prediction of future somatic activity for neuronal transfer and plasticity, Haider et al. (2021) also slightly alter the plasticity rule, which turns out to be crucial for the latent equilibrium mechanism. While the simulations by Sacramento et al. (2018) use the equations above, the new implementation [fill with neurips link](#) implicitly change them within its code. The fundamental building block of a network here is a layer, which is represented in code as an instance of the class `Layer`. Each instances holds information about its corresponding pyramidal- and interneurons. It also holds information about the synaptic connections between the two populations, as well as all incoming feedforward and feedback pyramidal synapses. A layer has two class methods that are fundamental to its computation; `update()` computes membrane potential derivatives and synaptic weight changes given pyramidal neuron activations from the previous and subsequent layers. `apply()` updates weights and membrane potentials from the previously calculated changes. Layers are processed in order from input to output layer, where all of them receive the `update()` signal first, before `apply()` is called on all of them. This ordering ensures, that changes in activation do not cascade through the layers and lead to excessive activations at the output. Yet, since next layer activations at time

$t$  have not been computed, top down information is always delayed by one timestep. **TODO: evaluate importance of this**

Thus, the equations for membrane updates change slightly:

$$\dot{W}_{ij}(t) = \eta(\phi(u_i) - \phi(\alpha v_i^{basal}(t)))\phi(u_j) \quad (2.70)$$

$$\Delta W_{ij}(t, T) = \int_t^T dt' \eta(\phi(u_i^{t'}) - \phi(\widehat{v}_i^{t'}))\phi(u_j^{t'}) \quad (2.71)$$

$$\Delta W_{ij}(t, T) = \eta \int_t^T dt' (\phi(u_i^{t'}) - \phi(\widehat{v}_i^{t'}))\phi(u_j^{t'}) \quad (2.72)$$

$$V_i^* = \phi(u_i^{t'}) - \phi(\widehat{v}_i^{t'}) \quad (2.73)$$

$$s_j^* = \kappa_s * s_j \quad (2.74)$$

## 2.10 Latent equilibrium

$$\phi(V^{som}) \rightarrow \phi(\check{V}^{som}) \quad (2.75)$$

$$\check{V} := V + \tau^m \dot{V} \quad (2.76)$$

$$(2.77)$$

$$\frac{d}{dt} W_{ba} = \eta(\phi(V_b^{som}) - \phi(\alpha V_b^{dend}))\phi(V_a^{som}) \quad (2.78)$$

$$\frac{d}{dt} W_{ba} = \eta(\phi(\check{V}_b^{som}) - \phi(\alpha \check{V}_b^{dend}))\phi(\check{V}_a^{som}) \quad (2.79)$$

## 2.11 rate neurons in NEST

## 2.12 simulation details/updates

All voltages need to be reset between simulations!

- injections into the network
- output layer readout
- interoperability of networks
-

# Chapter 3

## Results

**TODO:** Today, I changed the test criterion from the output neuron voltage at time  $t$  to a mean over a sample of the last  $20ms$ , network performance improved tremendously. Intuitively makes sense, but in particular it makes NEST networks diverge less after peak performance is reached. Are fluctuations in output layer activity increasing during late stages of training?

**TODO:** it might be worth experimenting with different synaptic delays in NEST in order to evaluate learning performance under biologically plausible transmission times. How easy this will assumably be to implement in NEST deserves note at this point.

**TODO:** talk about the fact that NEST synapses are updated, and SpikeEvents stored to ring buffers to be integrated into  $u_{som}$  after the synaptic delay. How much of physiological synaptic delays occurs pre- and postsynaptically in pyramidal neurons?

### 3.1 direct feedback connections to interneurons

Vaughn and Haas (2022); Mancilla et al. (2007)

### 3.2 Presentation times with latent equilibrium

In order to validate the performance of my implementations, I replicated a parameter study from Haider et al. (2021)[Fig. 3]. The results for the NEST network using spiking neurons with default parameters **TODO: elaborate on this** are shown in Figure 3.1. A



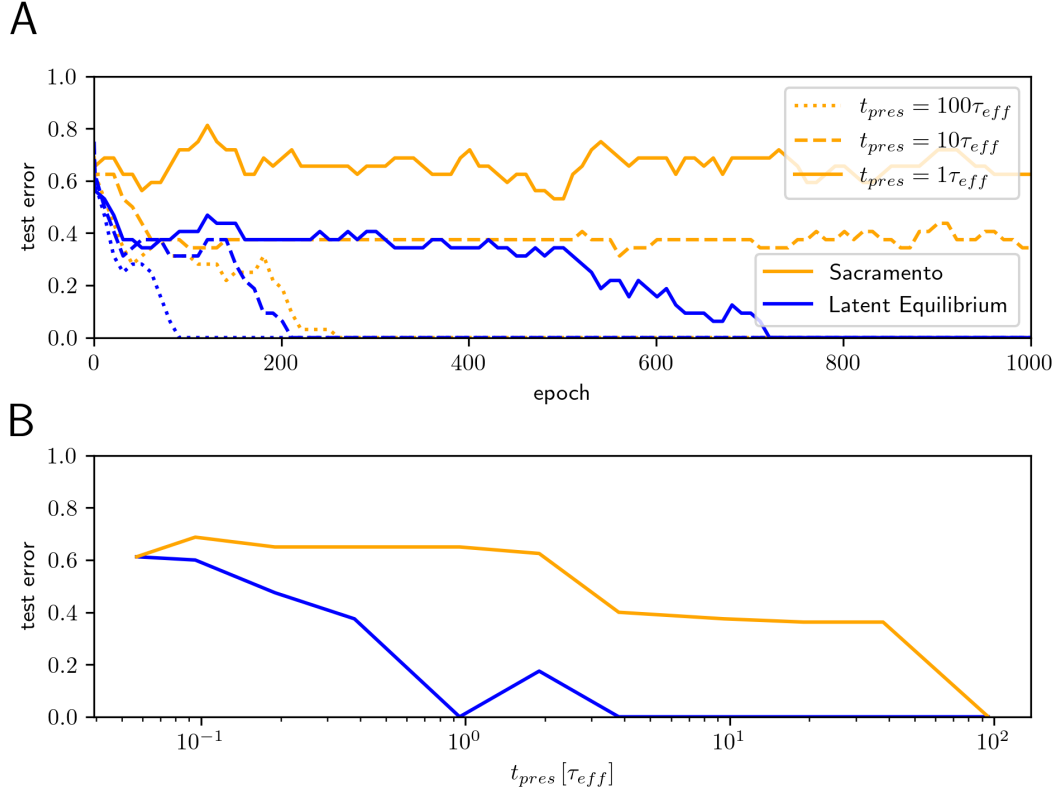


**Figure 3.1:** Replication of Figure 3 from Haider et al. (2021) using networks of spiking neurons in the NEST simulator. **A:** Comparison between Original pyramidal microcircuit network by Sacramento et al. (2018) and Latent equilibrium variant from Haider et al. (2021). Shown is the training of a network with 9-30-3 neurons on the 'Bars' Dataset from **TODO: describe it** with three different stimulus presentation times. **B:** Test performance after 1000 Epochs as a function of stimulus presentation time.

## Chapter 4

# room for random observations

- When reducing the `weight_scale` parameter weights converge to lower absolute levels. I.e. mean abs weight drops from 0.5 to approx 0.1
- When reducing the size of the bar dataset by just 1 element, much simpler networks are capable of learning the task at lower `t_pres`. Failure to learn shows strange behaviour: the network fails to predict any sample of one group, with the group which it fails to represent switching every now and then.
- increasing apical  $C_m$  for spiking neurons was a straight banger.
- I switched input neurons for `poisson_generators`. This is faster, but will fuck up any simulations that rely on precise spike timing, since the generator redraws spikes for every target `nrn`.

# Chapter 5

## Discussion

### 5.1 Limitations of the implementation

Network needs to be reset between stimuli original does not do that, in NEST it's kind of a big deal.

- exposure time and training set still quite large
- non-resetting, non-refractory

### 5.2 Whittington and Bogacz criteria

In which we discuss, to what extent the network conforms to the criteria for biologically plausible learning rules introduced by Whittington and Bogacz (2017):

1. Local computation. A neuron performs computation only on the basis of the inputs it receives from other neurons weighted by the strengths of its synaptic connections.
2. Local plasticity. The amount of synaptic weight modification is dependent on only the activity of the two neurons the synapse connects (and possibly a neuromodulator).
3. Minimal external control. The neurons perform the computation autonomously with as little external control routing information in different ways at different times as possible.
4. Plausible architecture. The connectivity patterns in the model should be consistent with basic constraints of connectivity in neocortex.

### 5.3 Should it be considered pre-training?

**TODO: someone said this network needs pre-training and that made me sad :(**

## 5.4 Relation to energy minimization

## 5.5 Outlook

This would likely be super efficient on neuromorphics!

I am not going to try plasticity with spike-spike or spike-rate dendritic errors  
reward-modulated urbanczik-senn plasticity?

## Chapter 6

# Appendix

### 6.1 Somato-dendritic coupling

Urbanczik and Senn (2014) discuss a possible extension to their neuron- and plasticity model, in which the dendro-somatic coupling transmits voltages in both directions. They show that the plasticity rule requires only minor adaptations for successful learning under this paradigm. Yet, as described by passive cable theory, the flow between neuronal compartments is dictated by their respective membrane capacitances. These are calculated from their membrane areas, which vastly differ in the case of pyramidal neurons. **TODO: find a nice citation for**

15,006 458

will not be considered here. The motivation is, that dendritic membrane area is

### 6.2 Presentation times and Latent Equilibrium

Exactly matching parameters and the training environment to those of existing implementations turned out to be a significant challenge. Particularly the way NEST handles signal transmissions made an exact numerical replication of results impossible, as discussed in Section **TODO: talk about timing differences**. In order to validate, that

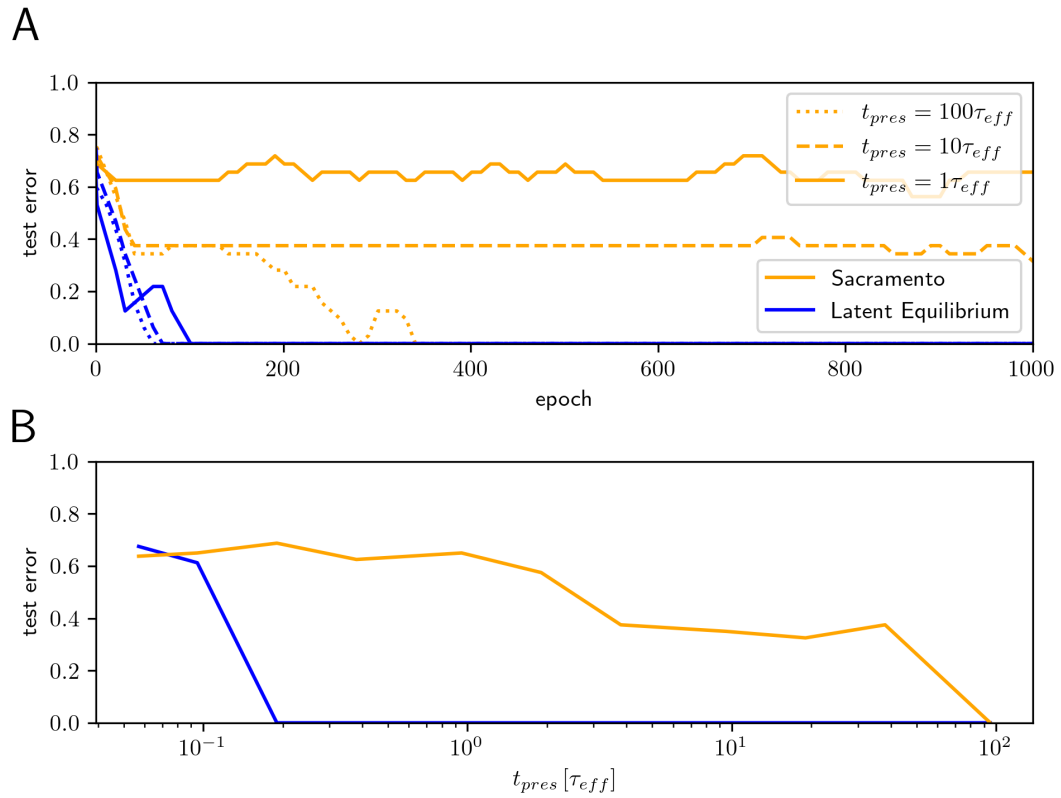


**Figure 6.1:** Replication of Figure 3.1 using a re-implementation of the Haider et al. (2021) code in python. Resulting performance matches the original results exactly, proving that my replication can serve as a baseline for comparing the NEST implementation

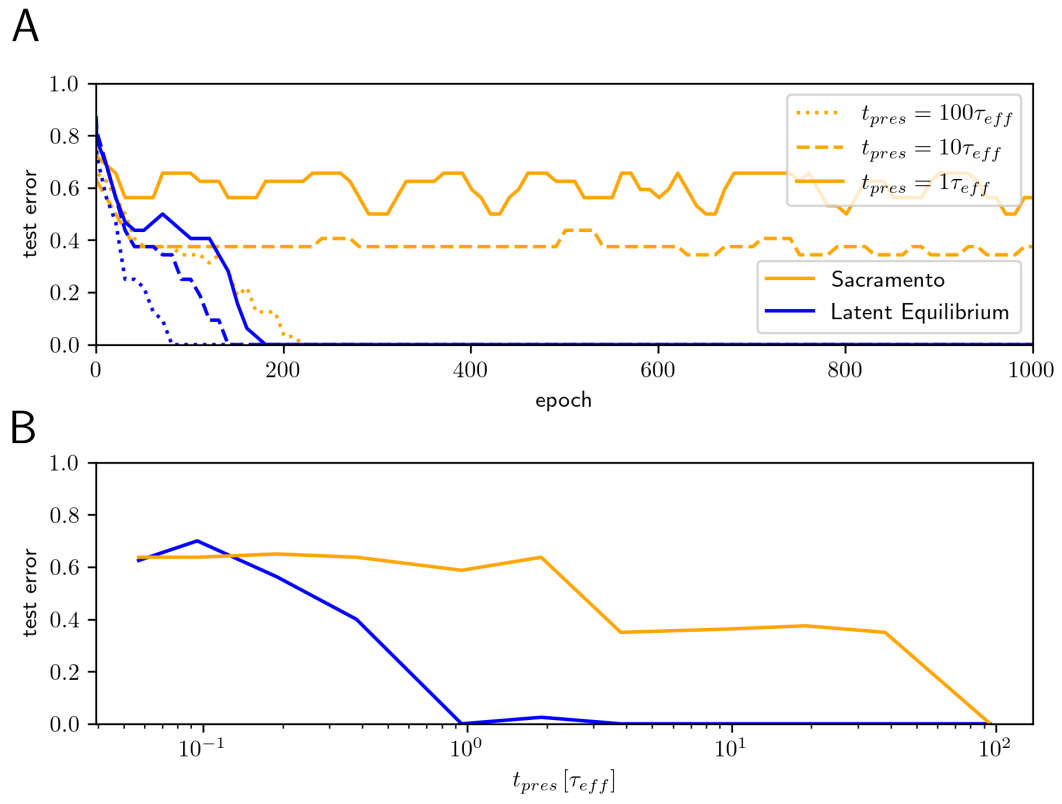


**Figure 6.2:** Replication of Figure 3.1 using networks of rate neurons in the NEST simulator.

1. In the torch implementation, there no persistence between timesteps at all. Input is fed into the network and processed feedforward and feedback. Output is read and weights (+biases) are updated. Rinse and repeat.
2. to what extent should dendritic and somatic compartments decay?
3. Can (should) we transfer the learned bias from the torch model?
4. I can "cheat" the apical voltage constraint for self prediction by increasing apical leakage conductance. How does this influence my model?
5. Is there some analytical approach to identifying why synaptic weights deviate from their intended targets?
6. I think that lambda needs to be scaled in dependence on  $g_{lk}$ , such that current inputs, spike inputs and leakage cancel each other out.
7. How do we deal with population size dependence?

### 6.3 Parameter study

- Transfer function  $\phi$
- interneuron mixing factor  $\lambda$
- injected current  $I_e$
- dendritic leakage conductance  $g_{lk,d}$
- somatic leakage conductance  $g_{lk,s}$
- Learning rate  $\eta$
- synaptic time constants  $\tau_{delta}$
- noise level  $\sigma$
- Simulation time  $\mathbb{T}$
- plasticity onset after the network relaxes
- compartment current decay  $\tau_{syn}$



## Observations

- In self-predicting paradigm, Apical errors stay constant, despite interneuron error steadily increasing.
- Interneuron error (between neuron pairs) is proportional to absolute somatic voltage in self-predicting paradigm.
- abs interneuron voltage is always higher than abs pyramidal voltage. This kind of makes sense, as interneurons receive direct current input proportional to pyramidal voltage in addition to feedforward input. This discrepancy disappears when setting  $\lambda$  to 0 as expected.
- When plasticity is enabled from a random starting configuration, apical error **sometimes** converges to better values than can be achieved in both self-predicting paradigms. I believe this to be a huge issue: the self-predicting state does not cause minimal apical voltage, and completely decayed feedback weights are preferable to perfectly counteracting feedback weights.
- feedforward weights tend to increase absolutely, i.e. drift towards the closest extreme. *This only happens since I re-implemented the second exponential term in the pyr\_synapse.* Yet they do not simply explode to the nearest extremum, but will traverse a zero weight to reach the maximum with equal sign as the weight they are supposed to match.
- feedback weights tend to decay to around zero. Yet they appear to remain close to zero in the direction they are supposed to be.
- Idea: I think that the somatic nudging is handled as straight currents being sent to the neuron, instead of the difference between actual and desired somatic voltage.
- In the paper and Mathematica code, Feedback learning rate is 2-5 times higher than feedforward lr. In my model, for learning to happen on similar time scales, feedback lr has to be 100 times lower than feedforward lr. An indicator that my plasticity is messed up.
- The simulation is likely producing way too few spikes (5-20 per 1000ms iteration). Could adapting the activation function yield better results?
- In the Mathematica solution, leakage conductance is greater than 1! ( $\delta U_i = -(g_L + g_D + g_{SI})U_i + g_D V_{BI} + g_{SI} U_Y$ ) with  $g_L + g_D + g_{SI} = 1.9$

## Chapter 7

# Preliminary structural components

### 7.1 Synaptic delays

Where I will inspect the implications of synaptic delays inherent to the NEST simulations on the model and plasticity rule. In particular, I will look at the biological necessity for this type of delay and discuss why any model attempting to replicate neuronal processes must be resilient to these delays.

### 7.2 Literature review - Backpropagation in SNN

Where I will review other attempts at implementing biologically plausible Backpropagation alternatives and contrast them to the current model.

### 7.3 NEST Urbanczik-senn implementation

### 7.4 My neuron model

- Low pass filtering
- multi-compartment computation
- Imprecision of the ODE
- abuse of the somatic conductance

#### 7.4.1 NEST rate neuron shenanigans

Given how long I worked on a rate neuron implementation in NEST, some pages should be devoted to this effort.

## 7.5 My synapse model

Where I discuss the synapse implementation with regard to multi-compartment neurons, urbanczik-archiving and in particular the issues with timing that arise from NEST delays.

## 7.6 The relation between the pyramidal microcircuit and actual microcircuits

Where I can finally use the shit that has been on my whiteboard for half a year...

This will also serve as valuable insight into how plausible this microcircuit actually is, and might give some insight into possible model extensions.

### 7.6.1 Interneurons and their jobs

## 7.7 Does it have to be backprop?

Where I will explain my concerns regarding the usefulness of approximating backpropagation in light of the substantial one-shot learning capability of the brain and the active inference model.

## 7.8 Discrepancies between mathematica and NEST model

1. Weights deviate slightly. This difference can be alleviated by exposing a single stimulus for a longer duration before switching.

## 7.9 Transfer functions

Where I will discuss the sensitivity of this entire simulation to minor changes in the parametrization and style of transfer function being used.

## Chapter 8

# The weight-leakage tradeoff

Where I will discuss the issue, that decreasing both synaptic weights and dendritic leakage conductance lead to more stability in the dendritic voltage, while at the same time requiring longer exposure per iteration.

### TODOs

- Prove that the network is stable in the self-predicting state and at the end of learning
- Show the limits of learning capability (i.e. how big of a network it can match)
- Test the network on a real-world dataset (mnist)
- prove/find literature on why the poisson process is a rate neuron in the limit.
- Does the network still learn when neurons have a refractory period?
- Comparison to other spiking backprops
- what can we learn from this? does it describe part of the brain

## Chapter 9

# Open Questions

- Any tips for transitioning to large simulation? also regarding the threadripper
- Is refractoryness interesting to us or more of a sidenote?
- Neuron dropout?
- How does one prove that the network is converged and will not diverge again.
- randomized/longer synaptic delays?
- As a follow up of dropout, maybe even neurogenesis?
- Should I look at delaying injection of the target activation?
- more ways in which this is biologically implausible?

$t_{pres}10 - 50\tau$

# Bibliography

- Bengio, Y., Lee, D.-H., Bornschein, J., Mesnard, T., and Lin, Z. (2015). Towards biologically plausible deep learning. *arXiv preprint arXiv:1502.04156*.
- Crick, F. (1989). The recent excitement about neural networks. *Nature*, 337(6203):129–132.
- Haider, P., Ellenberger, B., Kriener, L., Jordan, J., Senn, W., and Petrovici, M. A. (2021). Latent equilibrium: A unified learning theory for arbitrarily fast computation with arbitrarily slow neurons. *Advances in Neural Information Processing Systems*, 34:17839–17851.
- Liao, Q., Leibo, J., and Poggio, T. (2016). How important is weight symmetry in backpropagation? In *Proceedings of the AAAI Conference on Artificial Intelligence*, volume 30.
- Mancilla, J. G., Lewis, T. J., Pinto, D. J., Rinzel, J., and Connors, B. W. (2007). Synchronization of electrically coupled pairs of inhibitory interneurons in neocortex. *Journal of Neuroscience*, 27(8):2058–2073.
- Sacramento, J., Ponte Costa, R., Bengio, Y., and Senn, W. (2018). Dendritic cortical microcircuits approximate the backpropagation algorithm. *Advances in neural information processing systems*, 31.
- Stapmanns, J., Hahne, J., Helias, M., Bolten, M., Diesmann, M., and Dahmen, D. (2021). Event-based update of synapses in voltage-based learning rules. *Frontiers in neuroinformatics*, page 15.
- Urbanczik, R. and Senn, W. (2014). Learning by the dendritic prediction of somatic spiking. *Neuron*, 81(3):521–528.
- Vaughn, M. J. and Haas, J. S. (2022). On the diverse functions of electrical synapses. *Frontiers in Cellular Neuroscience*, 16.
- Whittington, J. C. and Bogacz, R. (2017). An approximation of the error backpropagation algorithm in a predictive coding network with local hebbian synaptic plasticity. *Neural computation*, 29(5):1229–1262.
- Whittington, J. C. and Bogacz, R. (2019). Theories of error back-propagation in the brain. *Trends in cognitive sciences*, 23(3):235–250.

- Yamins, D. L. and DiCarlo, J. J. (2016). Using goal-driven deep learning models to understand sensory cortex. *Nature neuroscience*, 19(3):356–365.